J Nat Med (2016) 70:75–88
DOI 10.1007/s11418-015-0939-z

ORIGINAL PAPER

Antiviral effects of Yinhuapinggan granule against influenza virus infection in the ICR mice model

Xue-qian Peng[1] · Hui-fen Zhou[1] · Yu-yan Zhang[1] · Jie-hong Yang[1] · Hai-tong Wan[2] · Yu He[3]

Received: 20 August 2015 / Accepted: 9 September 2015 / Published online: 6 October 2015

Abstract Yinhuapinggan granule (YHPG), a Chinese medicine granule based on Ma-Huang-Tang (Ephedra Decoction) and the clinical experience of Professor Wan Haitong, is used in traditional Chinese medicine (TCM) for the treatment of colds, influenza, fever, inflammation and cough. This study investigated the antiviral effects of YHPG on the production of inflammatory cytokines in influenza virus (IFV)-infected mice and evaluated the effect of YHPG on the expression of NF-κB p65 and the level of key signaling molecules in the TLR4 signaling pathway. ICR mice were orally administrated YHPG at doses of 7.5, 15 and 30 g kg^{-1} day^{-1} for 2 or 6 days after IFV infection. On days 3 and 7 after infection, YHPG (15 g/kg and 30 g/kg) significantly increased levels of interleukin (IL)-2 and interferon gamma and decreased levels of IL-4, IL-5 and tumor necrosis factor (TNF) in serum compared with the IFV control group. Furthermore, the expression of TLR4, MyD88, TRAF6 and NF-κB p65 at the mRNA and protein level was significantly lower in the YHPG (15 and 30 g/kg) treatment groups than in the IFV control group. These results suggest that YHPG has antiviral effects in IFV-infected mice, which is associated with the inhibition of the TLR4−MyD88−TRAF6 signaling pathway and the expression of NF-κB p65.

Keywords Yinhuapinggan granule · TLR4 · MyD88 · TRAF6 · NF-κB p65 · Antiviral effects

✉ Hai-tong Wan
whtong@126.com

✉ Yu He
heyu0923@hotmail.com

[1] Zhejiang Chinese Medical University, Hangzhou 310053, China

[2] Institute of Cardio-Cerebrovascular Diseases, Zhejiang Chinese Medical University, 548 Binwen Road, Hangzhou, China

[3] College of Pharmaceutical Science, Zhejiang Chinese Medical University, 548 Binwen Road, Hangzhou, China

Introduction

Influenza virus (IFV) is a negative-sense, single-stranded RNA virus that is a major cause of respiratory illness in humans [1]. Emerging evidence suggests that influenza infection triggers a massive inflammatory response that contributes to the development of pneumonia, which is a significant cause of morbidity and mortality [2, 3]. However, currently the licensed antiviral drugs available for prevention and treatment of influenza infection are M2 ion channel and neuraminidase inhibitors [4, 5]. Furthermore, because of possible side-effects and the rapid emergence of drug-resistant strains, the two classes of anti-influenza drugs are not effective in treating severe seasonal viral infections [6]. Consequently, the development of new antiviral agents is still urgently needed.

Toll-like receptors (TLRs) are a family of pattern recognition receptors that recognize pathogen-associated molecular patterns (PAMPs) associated with bacteria, viruses and fungi [7]. Of the TLRs, TLR4 is the primary receptor for lipopolysaccharides (LPSs) of Gram-negative bacteria and also recognizes the surface glycoproteins of enveloped viruses like RSV and IFV [8, 9]. The TLR4 signaling pathway is classified into two groups via two different intracellular adaptor proteins—myeloid differentiation factor 88 (MyD88)-dependent signaling and MyD88-independent/TRIF-dependent signaling [10]. In general, TLR4 binds to PAMPs to induce recruitment of

adaptor molecules to MyD88 through the TIR (Toll-IL-1R) domain after IFV infection. The interaction between the death domain of MyD88 and the corresponding domain in interleukin (IL)-1R-associated kinases leads to recruitment of downstream immune molecules like tumor necrosis factor (TNF) receptor-associated factor 6 (TRAF6), which results in activation of the NF-κB signaling pathway to activate innate immune responses against invading pathogens. However, studies have shown that activation of TLR4 contributes to exacerbated IFV pathogenesis and lung disease [11, 12]. In addition, pneumonia is associated with a progressive inflammatory response during IFV infection [13, 14]. Therefore, TLR4 is probably an important therapeutic approach for inflammatory response associated with influenza infection.

Traditional Chinese medicine (TCM), with a history of thousands of years, has been widely utilized for the treatment of infectious diseases, such as Ma-Huang-Tang (MHT) [15] and Ma-Xing-Shi-Gan-Tang (MXSGT) [16]. In contrast to most antiviral drugs which are comprised of one single chemical component, Chinese herbal medicines and their formulas are comprised of multiple components affecting multiple targets, which is of crucial importance in providing an effective and safe alternative to treat influenza infection. MHT (Ephedra Decoction), a TCM from the Treatise on Febrizle Disease of Zhang Zhongjing in the Han Dynasty, has been widely used to treat internal diseases such as influenza, bronchitis, asthma, and respiratory infection [17, 18]. Yinhuapinggan granule (YHPG) is an improved formula based upon the classical Ephedra decoction formula and the clinical experience of Professor Wan Haitong, which contains six Chinese herbs with a ratio of 4:4:4:2:2:1 (Table 1). Several ingredients of YHPG and their constituents have been reported to be effective against IFVs [19–26]. In our previous study, YHPG has the good effect of relieving cough, freeing lung and dispelling exogenous evils, clearing heat and resolving toxins [27, 28]. Furthermore, YHPG has been shown to inhibit the growth of IFV in vitro [29] and to inhibit IFV replication, alleviate damage to the lung and adjust for deviant immunologic functions in infected mice [30]. However, the mechanisms of YHPG are still unclear. In the present study, we investigated the effect of YHPG on the production of inflammatory cytokines in IFV-infected mice and evaluated the effect of YHPG on the expression of NF-κB and the level of key signaling molecules in the TLR4 signaling pathway.

Materials and methods

Herbs and reagents

Puerariae Lobatae Radix (batch number: 20131001), Flos Lonicerae Japonicae (batch number: 20131101), Polygoni Cuspidati Rhizoma (batch number: 20130801), Herba Ephedrae (batch number: 20130801), Armeniacae Semen Amarum (batch number: 20130801), and Glycyrrhizae Radix (batch number: 20131002) were purchased from Hangzhou Huadong Chinese Herbal Medicine Co., Ltd. (Hangzhou, China), and were identified by Prof. Shengwu Huang, College of Pharmaceutical Science, Zhejiang Chinese Medical University, where voucher specimens were deposited. The crude slices of these drugs conformed to quality standards in Chinese Pharmacopoeia (2010 edition).

Standards of L-ephedrine, D-pseudoephedrine (from Herba Ephedrae), glycyrrhizic acid (from Glycyrrhizae Radix), amygdalin (from Armeniacae Semen Amarum), chlorogenic acid (from Flos Lonicerae Japonicae), puerarin (from Puerariae Lobatae Radix), polydatin and emodin (from Polygoni Cuspidati Rhizoma) were purchased from the National Institute for the Control of Pharmaceutical and Biological Products (Beijing, China). Ribavirin granules (lot: 131165) were obtained from Baili Pharmaceutical Co., Ltd. (Sichuan, China). The BD^{TM} CBA Mouse Th1/Th2 Cyokine kit for IL-2, IL-4, IL-5, interferon gamma (IFN-γ) and TNF was supplied by BD Biosciences (San Diego, CA, USA). Mouse-anti-mouse monoclonal antibody for TLR4, rabbit-anti-mouse polyclonal antibody for MyD88 and rabbit-anti-mouse polyclonal antibody for TRAF6 were purchased from Novus Biologicals (CO, USA), and rabbit-

Table 1 Component herbs of YHPG

Pharmaceutical name	Botanical plant name	Family	Weight (g)	Used part
Flos Lonicerae Japonicae	*Lonicera japonica* Thunb.	Caprifoliaceae	10	Flower bud
Herba Ephedrae	*Ephedra sinica* Stapf.	Ephedraceae	5	Aerial part
Puerariae Lobatae Radix	*Pueraria lobata* (Willd.) Ohwi	Lamiaceae	10	Radix
Polygoni Cuspidati Rhizoma	*Polygonum cuspidatum* Sieb. et Zucc.	Polygonaceae	10	Root and rhizome
Armeniacae Semen Amarum	*Prunus armeniaca* L. var. ansu. Maxim.	Rosaceae	5	Fruit
Glycyrrhizae Radix	*Glycyrrhiza uralensis* Fischer	Leguminosae	2.5	Root and stolon

anti-mouse polyclonal antibody for NF-κB p65 was purchased from Santa Cruz Biotechnology (CA, USA).

Preparation of YHPG

YHPG granules (batch number: 20141101) were produced and supplied by Hangzhou Huadong Medicine Group Kangrun Pharmaceutical Co., Ltd. (Hangzhou, China). Briefly, the powdered Puerariae Lobatae Radix (1,000 g) and Flos Lonicerae Japonicae (1,000 g) were immersed in 10 L 70 % ethanol for 12 h and extracted using a heating reflux method at 85 °C twice (1 h each time). The two collected extractions were mixed, filtered and concentrated under reduced pressure to a relative density of 1.14 (50–60 °C) (solution A). The powdered Polygoni Cuspidati Rhizoma (1,000 g) was immersed in 10 L 80 % ethanol for 12 h and extracted using a heating reflux method at 85 °C twice (1 h each time). The extraction was mixed, filtered and concentrated under reduced pressure to a relative density of 1.13 (45–50 °C) (solution B). The powdered Herba Ephedrae (500 g) and Glycyrrhizae Radix (250 g) were soaked in 12.5 L water for 2 h, the mixture was decocted with the powdered Armeniacae Semen Amarum (500 g) three times (1 h each time). The decoction was filtered and concentrated to a relative density of 1.15 (50–60 °C) (solution C). Subsequently, solution A was mixed with solutions B and C. After spray drying, the drying powder was fully blended with cornstarch (150 g) and made into granules, providing 1.25 kg YHPG granules (yield 25.9 %, w/w). The YHPG granules were then sterilized and put into bags (6 g per bag).

High-performance liquid chromatography (HPLC) analysis of YHPG

HPLC analysis was performed using an Agilent 1200 HPLC system, including a G1322A on-line degasser, a G1311A quaternary pump, a G1316A column oven, a G1329A autosampler, and a G1315B photodiode array detector, controlled by an Agilent Rev. B.04.01 chemstation. Chromatographic separation was performed on an Agilent Eclipse XDB-C18 column (4.6 × 250 mm, 5 μm) at 35 °C. The photodiode array detector was set at 210 nm. The mobile phase was a mixture of water containing 0.1 % phosphoric acid (A) and acetonitrile (B). The linear gradients between the time points were 0–10 min at 3–9 % B, 10–25 min at 9–9 % B, 25–40 min at 9–20 % B, 40–65 min at 20–55 % B, 65–75 min at 55–70 % B, 75–80 min at 70–3 % B. The flow rate was maintained at 1.0 mL/min and the injection volume was 10 μL.

Virus

Mouse-adapted IFV A/PR/8/34 (H1N1) was donated by Professor Yi-yu Lu from the Zhejiang Center for Disease Control and Prevention, China. The virus was grown in the allantoic cavity of a 9-day-old embryonated egg for 48 h at 37 °C. The allantoic fluid was harvested and centrifuged at 1,000×g for 20 min, and the resulting supernatant, with hemagglutination titer 1024, was then stored in small portions at −80 °C. The Reed–Muench method was used to determined the LD_{50} of virus in mice ($LD_{50} = 10^{-3.5}$/0.02 mL).

Animals and experimental design

Male specific pathogen-free ICR mice, weighing 18–22 g, were obtained from the Animal Experimental Center, Zhejiang Chinese Medical University (laboratory animal certificate: scxk 2008-0016). Animals were housed in plastic cages in an air-conditioned room at 23 ± 2 °C with a relative humidity of 55 ± 10 % under a 12-h light/dark cycle, fed a standard laboratory diet and given water ad libitum. Animal experiments were carried out in accordance with local guidelines for the care of laboratory animals of Animal Experimental Center, Zhejiang Chinese Medical University, and were approved by the ethics committee for research on laboratory animal use at the institution.

The mice were randomly divided (20 mice each group) into experimental groups, normal control group (Normal-C) and IFV-infected control group (IFV-C). Mice were intranasally inoculated with 15 LD_{50} doses of IFV in 20-μL sterile saline except for the Normal-C group. One hundred and fifty grams of YHPG granules were dissolved in 100 mL of distilled water and diluted to the desired concentrations before use. After 2-h inoculation, YHPG (7.5, 15, and 30 g/kg) or ribavirin (75 mg/kg) was orally administered to the experimental groups daily for 2 or 6 days, respectively. Mice in the IFV-C and Normal-C groups were treated with normal saline at the same intervals. The low dose of YHPG for the animal (mouse) study was equivalent to the human dosage in clinical practice, while the moderate and high doses of YHPG were two and four times the human clinical dosage, respectively. On the third and seventh day after IFV infection, ten mice from each group were killed to collect serum and lung tissues. The serum was stored at −20 °C and lung tissues were divided into two parts—the right lung for immunohistochemical analysis and the left lung for RT-PCR analysis.

Determination of cytokines in serum by flow cytometry

IL-2, IL-4, IL-5, IFN-γ and TNF levels in serum were measured using Becton Dickson Cytometric Bead Array (CBA) Mouse Th1/Th2 Cyokine kit as per the manufacturer's instructions. Briefly, 50 μL of the mixed capture beads were added to all assay tubes containing the control tubes and test assay tubes. Fifty microliters of each test sample and the mouse Th1/Th2 cytokine standard dilutions were transferred into the test assay tubes and the control tubes, respectively. Then, 50 μL of the mouse Th1/Th2 PE detection reagents was added to all assay tubes and incubated for 2 h at room temperature in darkness. One milliliter of wash buffer was added to each assay tube and centrifuged at 200×*g* for 5 min. After carefully aspirating and discarding the supernatant from each assay tube, the bead pellet was resuspended in 300 μL wash buffer and analysed using FACSCalibur cytometer (BD Biosciences) and BD CellQuest Pro software (BD Biosciences) [31].

Real-time RT-PCR analysis

The left lung from each mouse was homogenized in precooled normal saline and centrifuged at 1466×g for 10 min at 4 °C. Total RNA in the supernatant was extracted with RNA Qiagen reagent (Qiagen, Hilden, Germany), and dissolved in DEPC-H_2O (30 μL). The total RNA was reverse transcribed with PrimeScript™ RT Master Mix kit (Takara Bio, Shiga, Japan). Real-time RT-PCR was performed on cDNA samples using the SYBR® Premix Ex Tap™ II (Takara Bio). The primers were synthesized by Sangon Biotech, Co., Ltd. (Shanghai, China) and are described in Table 2. The reaction conditions were 95 °C 2 min, followed by 95 °C 15 s, 55 °C 35 s for 40 cycles using a QuanStudio 12 K Flex Real-time PCR System (Applied Biosystems®; Thermo Fisher Scientific, Waltham, MA, USA). The relative quantification of PCR products was performed according to the $2^{-\Delta\Delta Ct}$ method [32]. The fold change in target gene cDNA relative to the GAPDH internal control was determined using the following formula:

$$\text{Fold change} = 2^{-\Delta\Delta CT},$$
$$\text{where } \Delta\Delta Ct = \left(Ct_{\text{target gene}} - Ct_{GAPDH}\right) - \left(Ct_{\text{control}}\ Ct_{GAPDH}\right)$$

Immunohistochemical analysis

On day 3 and day 7 after IFV infection, the right lung lobes from each mouse were washed with normal saline, fixed with 10 % formaldehyde solution, and embedded in paraffin. For immunohistochemical analysis, paraffin-embedded lung sections (3 μm) were rinsed with 3 % H_2O_2 for 10 min to block endogenous peroxide activity and treated with sodium citrate buffer (pH 6.0) in a 500 W microwave oven for 15 min for antigen retrieval. After blocking the nonspecific antigen with normal goat serum, the sections were then incubated with primary antibody of TLR4 (mouse-anti-mouse monoclonal antibody, 1:150), MyD88 (rabbit-anti-mouse polyclonal antibody, 1:75), TRAF6 (rabbit-anti-mouse polyclonal antibody, 1:1,500) or NF-κB p65 (rabbit-anti-mouse polyclonal antibody, 1:100) at room temperature for 60 min. The sections were washed 3 times for 5 min each in PBS and then incubated with secondary antiserum (EnVision Two-Step kit; Dako, Glostrup, Denmark) for 40 min at room temperature. Subsequently, the lung sections were washed 3 times with PBS and then incubated with diaminobenzidine and hematoxylin staining solution (Harris) for 2–3 min, and dehydrated using graded alcohols and xylene. Finally, the brown reaction product was observed at 200× magnification using a light microscope and the number of positive cells in five randomly chosen fields was counted. Furthermore, the immunoreactivity of the target proteins was quantified based on the integrated optical density (IOD) of immunostaining per field using Image-ProPlus 6.0 software (Media Cybernetics, USA).

Statistical analysis

All data were presented as mean ± SD. Statistical analysis was performed with two-tailed indirect Student tests with SPSS17.0 for Windows (SPSS, Inc., Chicago, IL, USA). Statistical analysis for multiple group comparisons was performed by one-way ANOVA with Bonferroni's

Table 2 Primer sequences used for RT-PCR analysis

Gene	Product size (bp)	Forward (5′-3′)	Reverse (5′-3′)
TLR4	101	GCACTGACACCTTCCTTTCC	GCCTTAGCCTCTTCTCCTTCA
MyD88	136	TGGTGGTTGTTTCTGACGAT	GGAAAGTCCTTCTTCATCGC
TRAF6	119	GAGGTCACGAGCCACTTCTT	ACAGACAGATGAGCCACAGG
NF-κB P65	185	TCAATGGCTACACAGGACCA	TCGCTTCTTCACACACTGGA
GAPDH	141	GCAAGTTCAACGGCACAG	CGCCAGTAGACTCCACGAC

corrections. Differences were considered statistically significant when $p < 0.05$.

Results

HPLC profile of YHPG

As compared with standard reference compounds, eight effective constituents of YHPG, including L-ephedrine, D-pseudoephedrine, chlorogenic acid, amygdalin, puerarin, polydatin, glycyrrhizic acid and emodin, were analyzed by HPLC (Fig. 1). The contents of these compounds in YHPG were 0.73, 0.407, 1.92, 6.37, 4.35, 1.79, 0.692, 0.329, respectively.

Effects of YHPG on the levels of IL-2, IL-4, IL-5, IFN-γ and TNF in serum

The levels of IL-2, IL-4, IL-5, IFN-γ and TNF in serum were measured by cytometric bead array. As shown in Fig. 2, on days 3 and 7 after infection, the levels of IL-2, IL-4, IL-5, IFN-γ and TNF in the IFV-C group were significantly higher than in the Normal-C group ($P < 0.01$). Compared with the IFV-C group, ribavirin and YHPG (15 and 30 g/kg) significantly increased levels of IL-2 and IFN-γ and decreased levels of IL-4, IL-5 and TNF in serum on days 3 and 7 after infection ($P < 0.01$ or $P < 0.05$). However, there was no significant difference in cytokine expression between the YHPG (7.5 g/kg) and IFV-C groups.

Effects of YHPG on the mRNA expression of the TLR4 signaling pathway

TLR4, MyD88, TRAF6 and NF-κB p65 mRNA expression in lung tissue was detected by RT-PCR. As shown in Fig. 3, TLR4, MyD88, TRAF6 and NF-κB p65 mRNA expression in the IFV-C group was significantly upregulated on days 3 and 7 after infection ($P < 0.01$) compared with the Normal-C group. Ribavirin and YHPG (15 and 30 g/kg) significantly downregulated TLR4, MyD88, TRAF6 and NF-κB p65 mRNA expression in comparison to the IFV-C group on days 3 and 7 after infection ($P < 0.01$ or $P < 0.05$). However, there was no significant difference in mRNA expression between the YHPG (7.5 g/kg) and IFV-C groups.

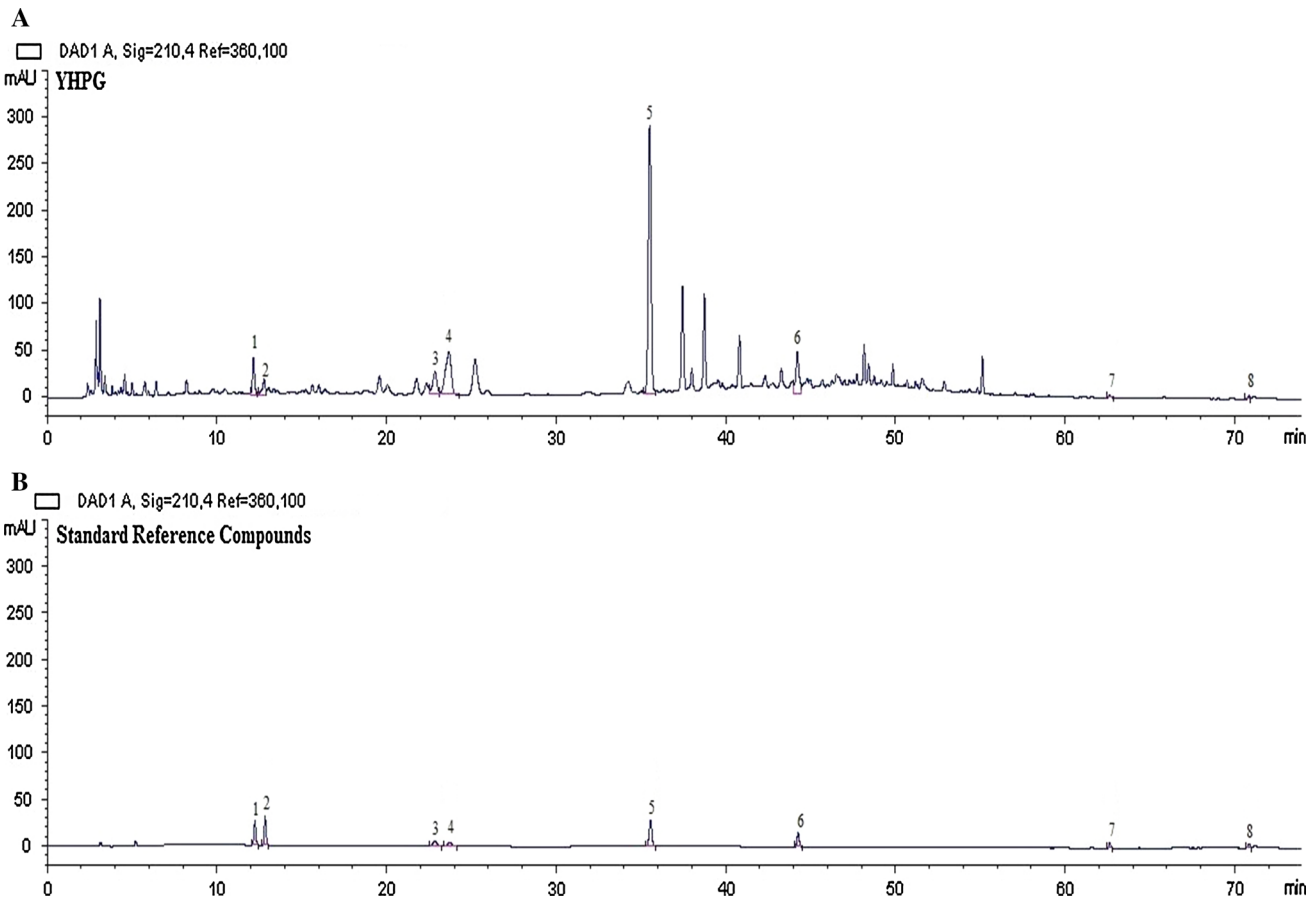

Fig. 1 Two-dimensional HPLC chromatograms of eight effective constituents inYHPG at 210 nm. *1* L-ephedrine; *2* D-pseudoephedrine; *3* chlorogenic acid; *4* amygdalin; *5* puerarin; *6* polydatin; *7* glycyrrhizic acid and *8* emodin

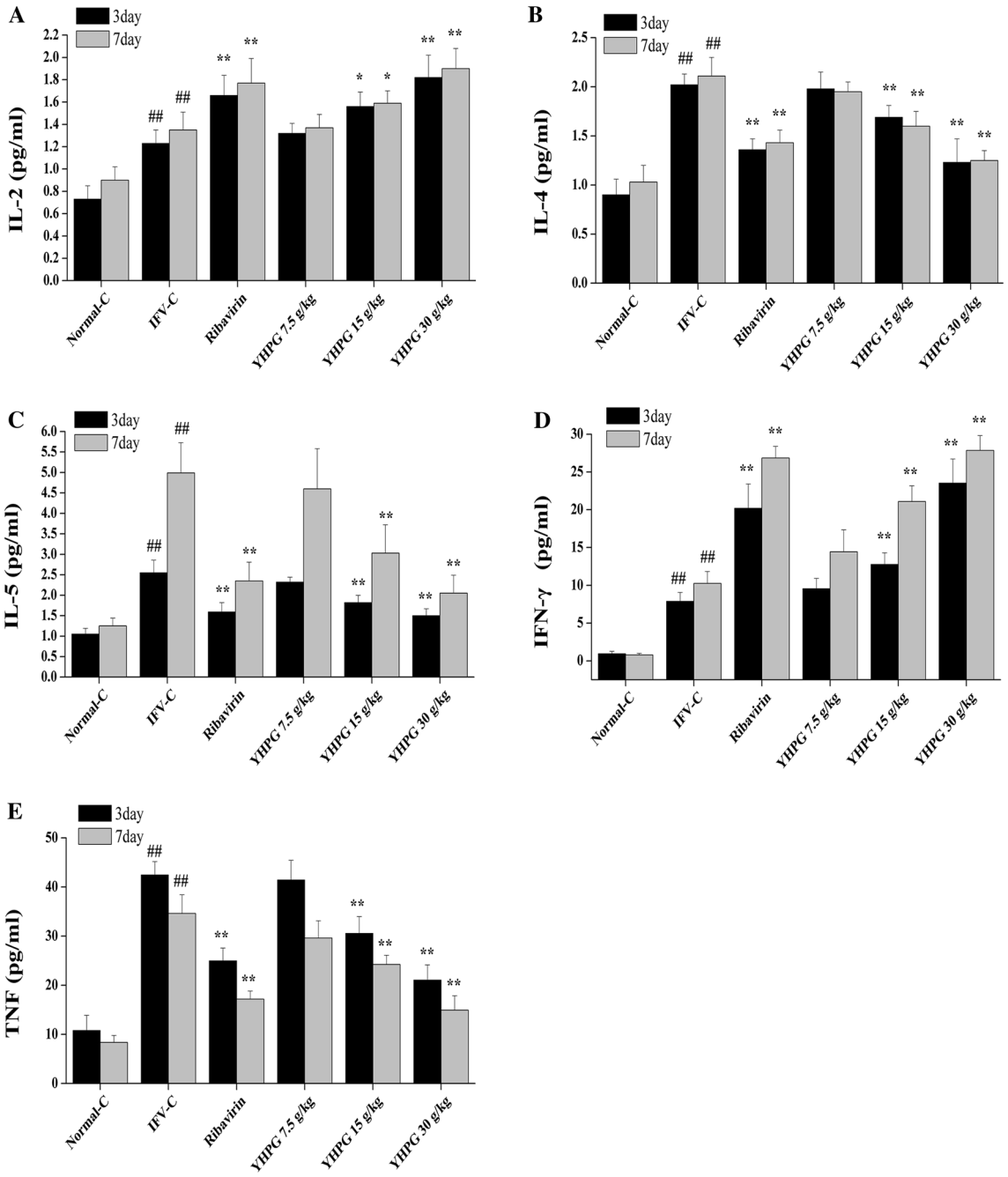

Fig. 2 Effects of YHPG on levels of IL-2 (**a**), IL-4 (**b**), IL-5 (**c**), IFN-γ (**d**) and TNF (**e**) in serum on days 3 and 7 after infection ($n = 10$ in each group). All data are presented as mean ± SD. *Asterisks* denote the significant levels: $^{\#\#}$ $P < 0.01$ vs. Normal-C,* $P < 0.05$, ** $P < 0.01$ vs. IFV-C

Effects of YHPG on the protein expression of the TLR4 signaling pathway

Immunohistochemical determination of TLR4, MyD88, TRAF6 and NF-κB p65 was performed to determine the effects of YHPG on the TLR4/MyD88-mediated NF-κB signaling pathway. We measured the IOD of TLR4, MyD88, TRAF6 and NF-κB p65 and calculated the mean values and SDs. As shown in Fig. 4, immunohistochemical analysis showed that the expression of TLR4 protein in the IFV-C group was significantly higher than in the Normal-C group on days 3 and 7 after infection ($P < 0.01$). Compared with the IFV-C group, ribavirin and YHPG (15 and 30 g/kg) significantly downregulated the protein

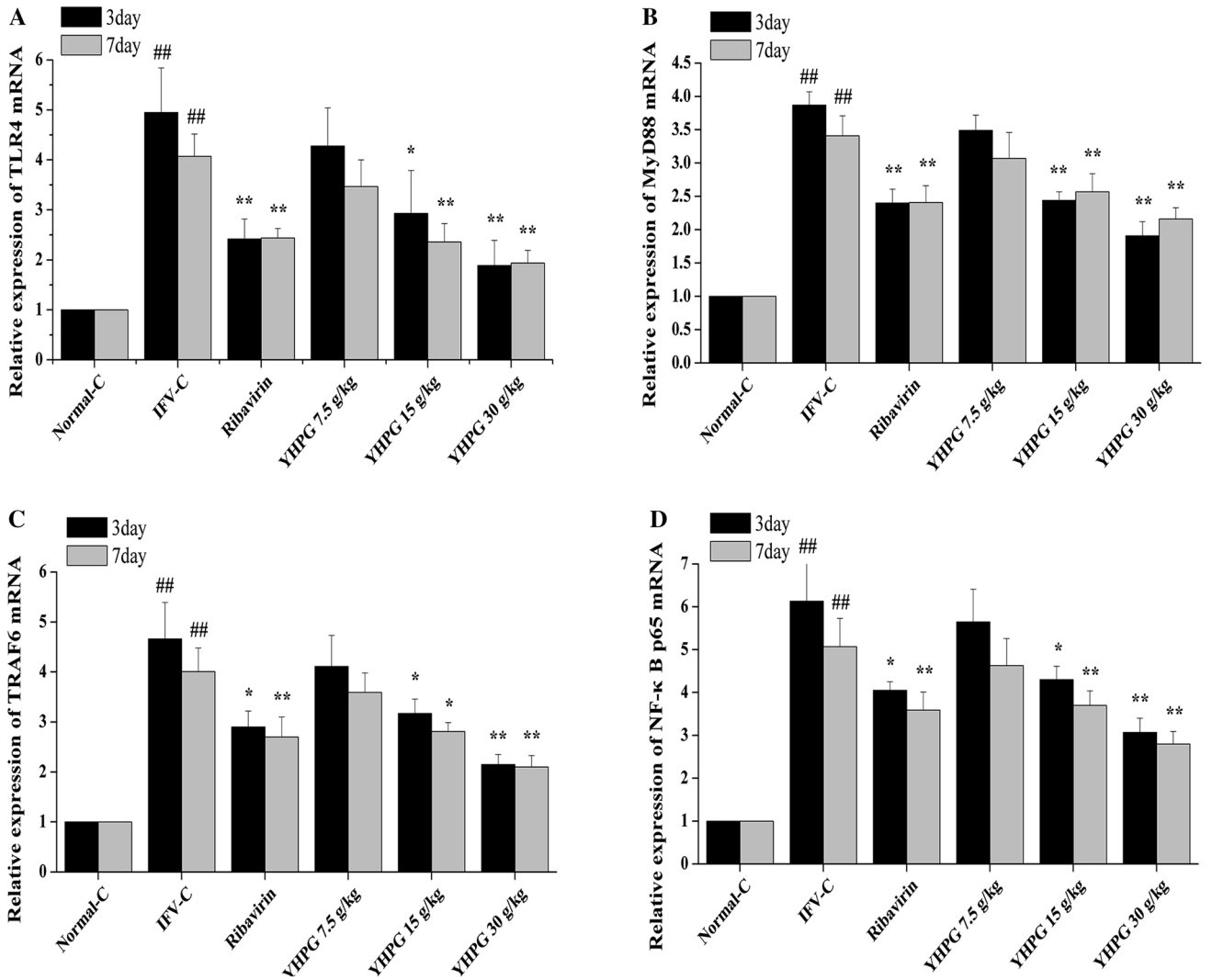

Fig. 3 Effects of YHPG on mRNA expression of TLR4 (**a**), MyD88 (**b**), TRAF6 (**c**) and NF-κB p65 (**d**) in lung tissue on days 3 and 7 after infection ($n = 10$ in each group). All data are presented as mean ± SD. *Asterisks* denote the significant levels: $^{\#\#}$ $P < 0.01$ vs. Normal-C, * $P < 0.05$, ** $P < 0.01$ vs. IFV-C

expression of TLR4 on days 3 and 7 after infection ($P < 0.01$). However, there was no significant difference in protein expression between the YHPG (7.5 g/kg) and IFV-C groups. These results are in accordance with the effects of YHPG on the mRNA expression of TLR4.

As shown in Fig. 5, the expression of MyD88 protein in the IFV-C group was significantly higher than in the Normal-C group on days 3 and 7 after infection ($P < 0.01$). Compared with the IFV-C group, ribavirin and YHPG (15 and 30 g/kg) significantly decreased the protein expression of MyD88 on days 3 and 7 after infection ($P < 0.01$). However, there was no significant difference in protein expression between the YHPG (7.5 g/kg) and IFV-C groups. These results are in accordance with the effects of YHPG on the mRNA expression of MyD88.

As shown in Fig. 6, the expression of TRAF6 protein in the IFV-C group was significantly higher than in the Normal-C group on days 3 and 7 after infection ($P < 0.01$). Compared with the IFV-C group, ribavirin and YHPG (15 and 30 g/kg) significantly downregulated the protein expression of TRAF6 on days 3 and 7 after infection ($P < 0.01$ or $P < 0.05$). However, there was no significant difference in protein expression between the YHPG (7.5 g/kg) and IFV-C groups. These results are in accordance with the effects of YHPG on the mRNA expression of TRAF6.

As shown in Fig. 7,the expression of NF-κB p65 protein in the IFV-C group was significantly higher than in the Normal-C group on days 3 and 7 after infection ($P < 0.01$). Compared with the IFV-C group, ribavirin and YHPG (15 and 30 g/kg) significantly downregulated the protein

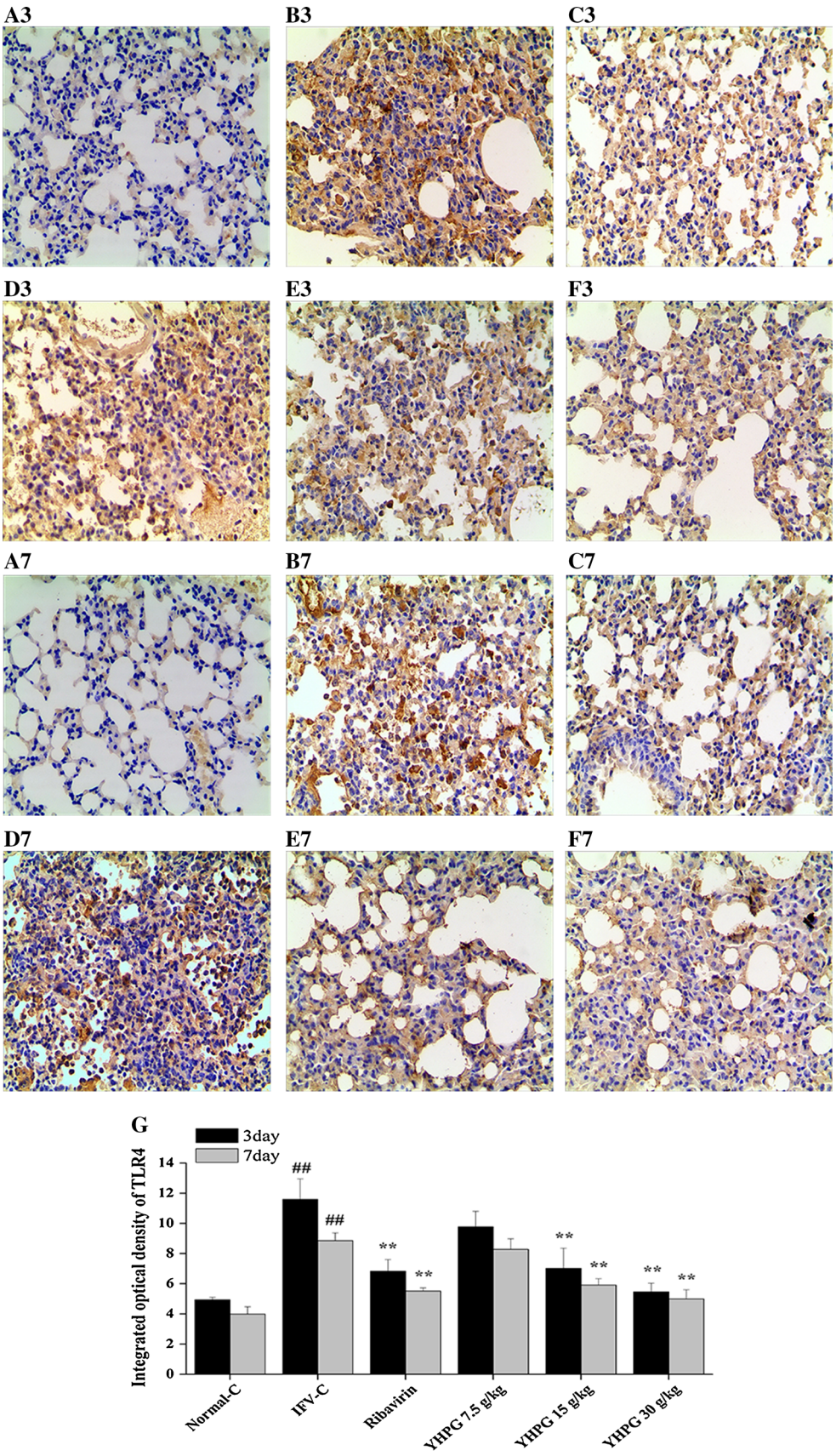

Fig. 4 Immunostaining microphotographs of TLR4 proteins in the lung tissues of IFV-infected mice (magnification 200×). **a** Normal control group (Normal-C), **b** IFV-infected control group (IFV-C), **c** infected mice treated with ribavirin (75 mg/kg) (Ribavirin), **d** infected mice treated with YHPG (7.5 g/kg) (YHPG 7.5 g/kg), **e** infected mice treated with YHPG (15 g/kg) (YHPG 15 g/kg), and **f** infected mice treated with YHPG (30 g/kg) (YHPG 30 g/kg). The numbers 3 and 7 refer to days 3 and 7 after infection, respectively. **g** Quantitative image analysis of TLR4 proteins was performed based on the integrated optical density (IOD) of positive immunostaining (*brown*) in the lung tisssues. All data are presented as mean ± SD ($n = 10$ in each group). *Asterisks* denote the significant levels: $^{\#\#} P < 0.01$ vs. Normal-C, $^{*} P < 0.05$, $^{**} P < 0.01$ vs. IFV-C

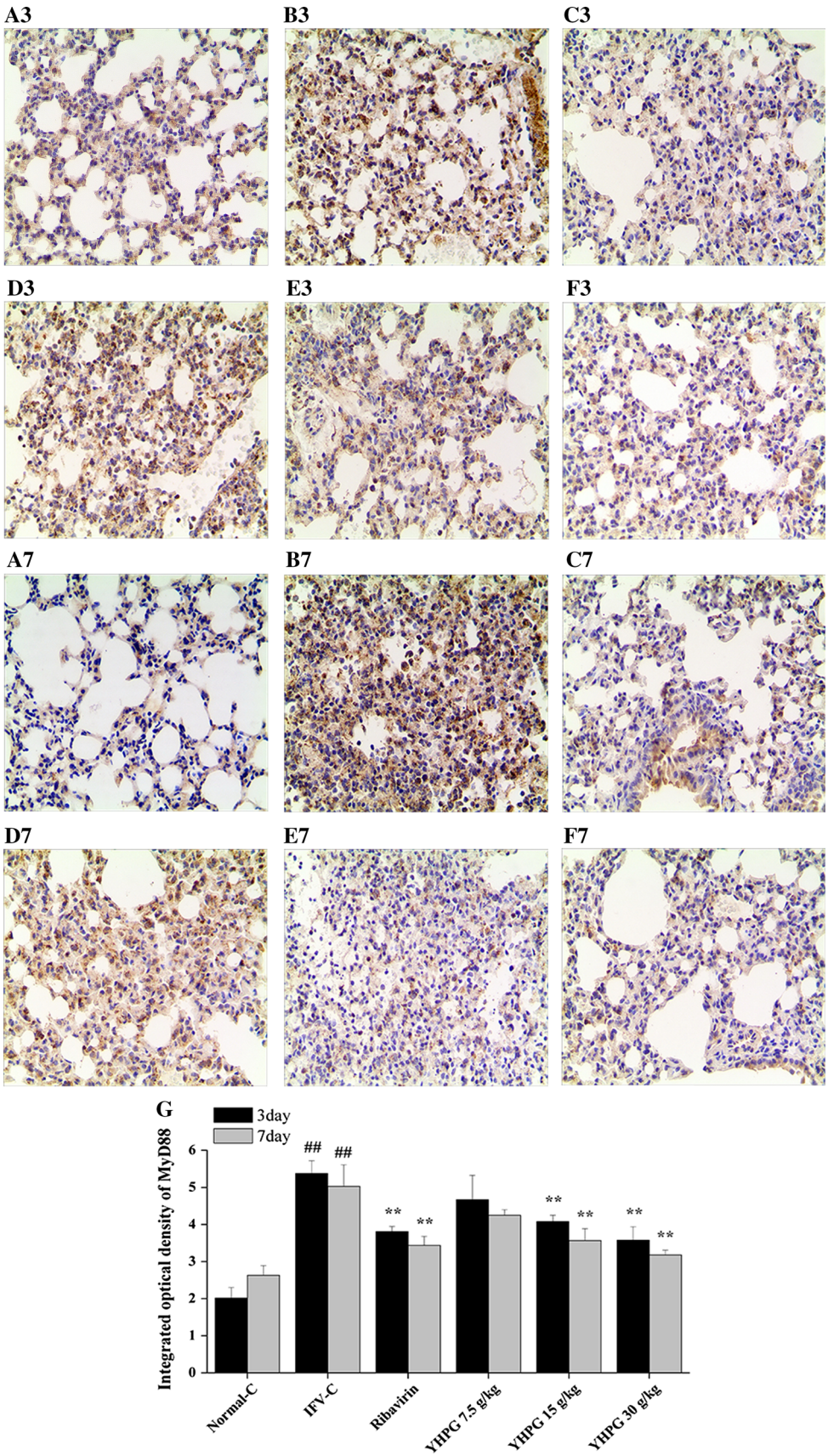

Fig. 5 Immunostaining microphotographs of MyD88 proteins in the lung tissues of IFV-infected mice (magnification 200×). **a** Normal control group (Normal-C), **b** IFV-infected control group (IFV-C), **c** infected mice treated with ribavirin (75 mg/kg) (Ribavirin), **d** infected mice treated with YHPG (7.5 g/kg) (YHPG 7.5 g/kg), **e** infected mice treated with YHPG (15 g/kg) (YHPG 15 g/kg), and **f** infected mice treated with YHPG (30 g/kg) (YHPG 30 g/kg). The numbers 3 and 7 refer to days 3 and 7 after infection, respectively. **g** Quantitative image analysis of MyD88 proteins was performed based on the integrated optical density (IOD) of positive immunostaining (*brown*) in the lung tisssues. All data are presented as mean ± SD ($n = 10$ in each group). *Asterisks* denote the significant levels: $^{\#\#} P < 0.01$ vs. Normal-C, * $P < 0.05$, ** $P < 0.01$ vs. IFV-C

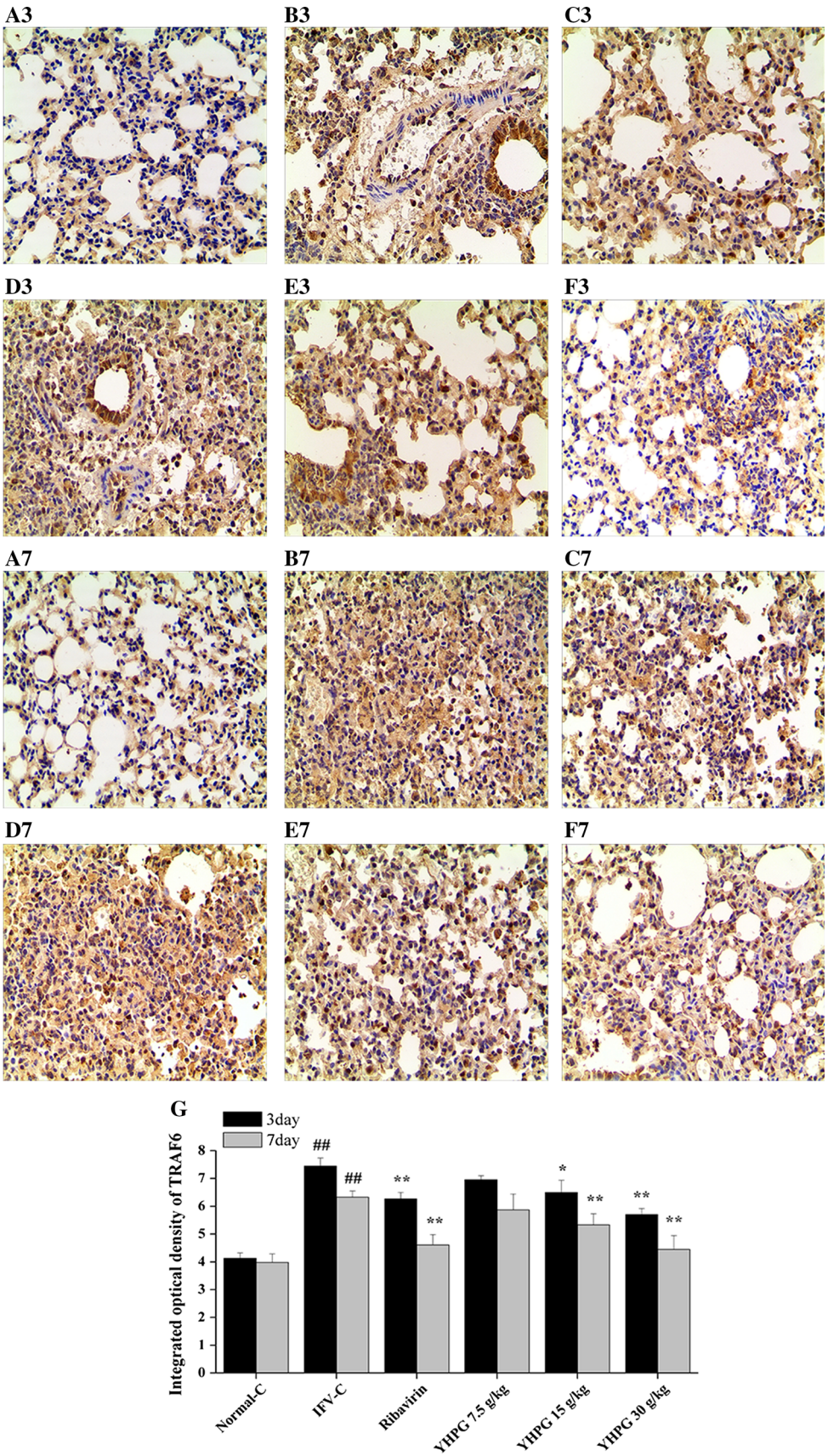

Fig. 6 Immunostaining microphotographs of TRAF6 proteins in the lung tissues of IFV-infected mice (magnification 200×). **a** Normal control group (Normal-C), **b** IFV-infected control group (IFV-C), **c** infected mice treated with ribavirin (75 mg/kg) (Ribavirin), **d** infected mice treated with YHPG (7.5 g/kg) (YHPG 7.5 g/kg), **e** infected mice treated with YHPG (15 g/kg) (YHPG 15 g/kg), and **f** infected mice treated with YHPG (30 g/kg) (YHPG 30 g/kg). The numbers 3 and 7 refer to days 3 and 7 after infection, respectively. **g** Quantitative image analysis of TRAF6 proteins was performed based on the integrated optical density (IOD) of positive immunostaining (*brown*) in the lung tisssues. All data were presented as mean ± SD ($n = 10$ in each group). *Asterisks* denote the significant levels: $^{\#\#}$ $P < 0.01$ vs. Normal-C, * $P < 0.05$, ** $P < 0.01$ vs. IFV-C

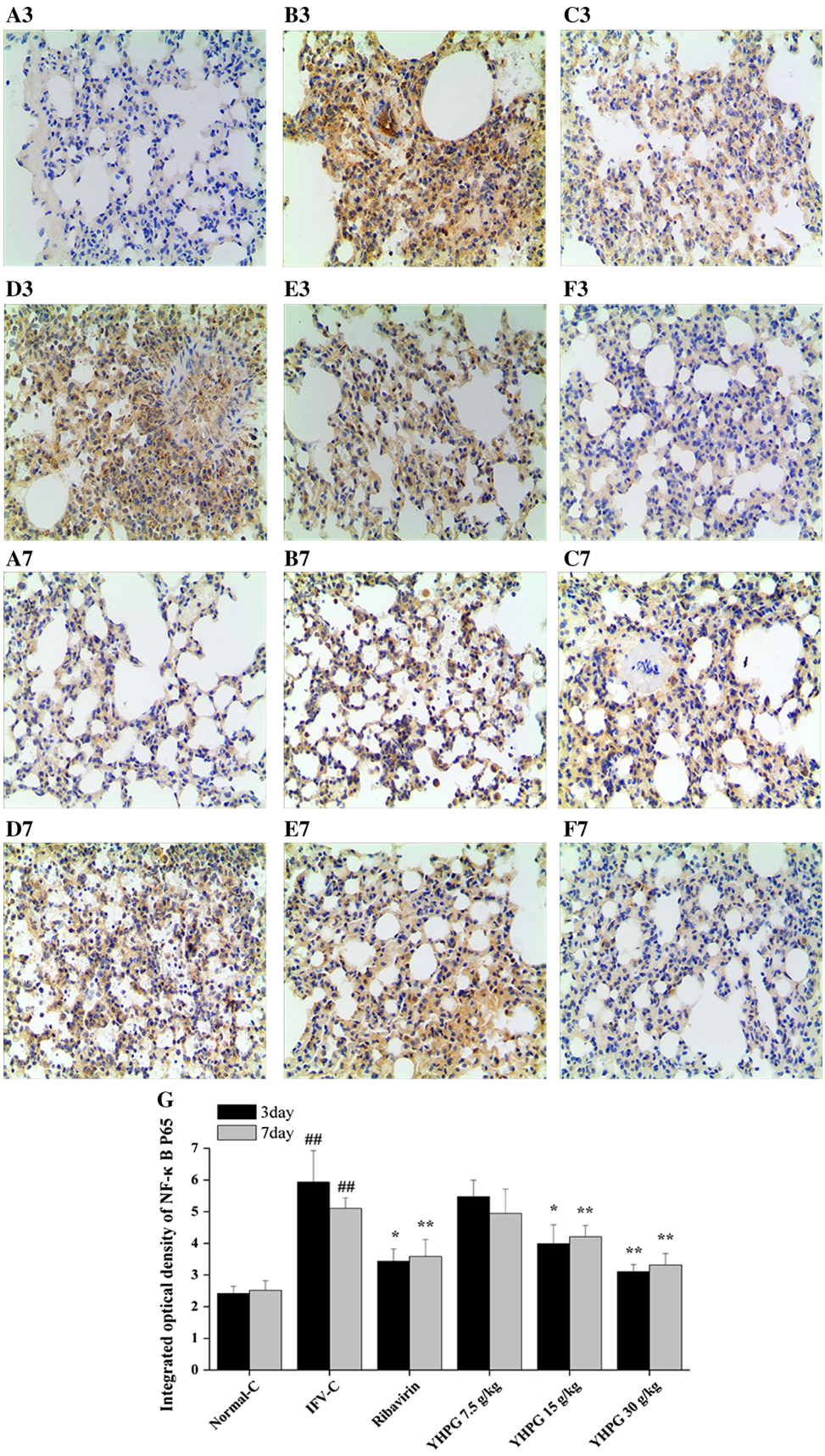

Fig. 7 Immunostaining microphotographs of NF-κB p65 proteins in the lung tissues of IFV-infected mice (magnification 200×). **a** Normal control group (Normal-C), **b** IFV-infected control group (IFV-C), **c** infected mice treated with ribavirin (75 mg/kg) (Ribavirin), **d** infected mice treated with YHPG (7.5 g/kg) (YHPG 7.5 g/kg), **e** infected mice treated with YHPG (15 g/kg) (YHPG 15 g/kg), and **f** infected mice treated with YHPG (30 g/kg) (YHPG 30 g/kg). The numbers 3 and 7 refer to days 3 and 7 after infection, respectively. **g** Quantitative image analysis of NF-κB p65 proteins was performed based on the integrated optical density (IOD) of positive immunostaining (*brown*) in the lung tisssues. All data are presented as mean ± SD ($n = 10$ in each group). *Asterisks* denote the significant levels: $^{\#\#}$ $P < 0.01$ vs. Normal-C, * $P < 0.05$, ** $P < 0.01$ vs. IFV-C

expression of NF-κB p65 on days 3 and 7 after infection ($P < 0.01$ or $P < 0.05$). However, there was no significant difference in protein expression between the YHPG (7.5 g/kg) and IFV-C groups. These results are in accordance with the effects of YHPG on the mRNA expression of NF-κB p65.

Discussion

Influenza can cause widespread infection and affect millions of people every year globally. The emergence of drug-resistant viruses has led to a need for the development of novel and effective antiviral agents [6, 33]. TCM, such as MHT, has become one of the popular choices for the treatment of influenza in China, because of its multiple pathways, multi-targets, and minimal side-effects [15]. YHPG is a Chinese medicine granule whose major ingredients are based upon the classical MHT formula. Modified prescriptions of MHT work perfectly for internal diseases such as influenza, bronchitis, asthma, respiratory infection [17]. Previous studies have demonstrated that YHPG has obvious antiviral effects in vitro [29] and inhibits IFV replication, alleviating damage to the lung and adjusting for deviant immunologic functions of infected mice [30]. However, the mechanism of YHPG against IFV is not fully understood.

It has been reported that the levels of cytokines are associated with symptom formation and host defenses in influenza [34, 35]. Although cytokines contribute to the elimination of pathogens, their excessive production can in turn result in tissue injury [36]. In the present study, we found that the levels of IL-2, IL-4, IL-5, IFN-γ and TNF in the IFV-infected mice were significantly higher than in the Normal-C group on days 3 and 7 after infection, suggesting that influenza infection triggers inflammatory responses resulting in the production of cytokines and chemokines. Consistent with previous studies [37, 38], YHPG (15 g/kg and 30 g/kg) treatment effectively increased levels of IL-2 and IFN-γ, while the levels of IL-4, IL-5 and TNF were decreased compared to the IFV-C group on days 3 and 7 after infection. IL-2 is a T-helper 1 (Th1) cytokine that stimulates IFN-γ secretion, which is crucial for viral clearance [39]. IFN-γ, which is produced by T cells and natural killer cells, protects infected mice from death at the early stage of IFV infection [40, 41]. Interestingly, we found that the increase in the level of IL-2 was synergistically associated with the level of IFN-γ in this study, which may be one aspect of the protective effect of YHPG. The TNF-α level is directly related with the severity of histologic lung lesions after infection [42]. In addition, TNF-α is a multifunctional inflammatory cytokine that is associated with morbidity during IFV infection [43]. Therefore, the effect of YHPG against influenza infection is likely to decrease inflammatory responses by modulating the expression of inflammatory cytokines (Fig. 7).

TLR4 is expressed in a variety of immune and non-immune cells, and plays an important role in the induction and regulation of immune and inflammatory responses to Gram-negative bacteria and IFV infection [8, 9]. Previous studies have demonstrated that TLR4 is a key contributor to influenza A-induced lung injury [44]. MyD88 is a crucial adaptor protein in TLR4 signaling, which is essential for proinflammatory cytokine production [45]. TRAF6 has been identified as a signal transducer, which is recruited by the adaptor MyD88 to activate the NF-κB signaling pathway, resulting in the production of cytokines [46, 47]. Furthermore, the production of inflammatory cytokines is regulated by the transcription factor NF-κB, which plays a crucial role in immune and inflammatory responses [48]. Therefore, TLR4, MyD88, TRAF6 and NF-κB expression in lung tissue was detected by RT-PCR and immunohistochemistry. Our results showed that TLR4, MyD88, TRAF6 and NF-κB expression at the mRNA and protein level in the IFV-C group was significantly higher than in the Normal-C group on days 3 and 7 after infection, suggesting that activation of TLR4 can induce expression of its downstream gene after IFV infection. Compared with the IFV-C group, YHPG (15 and 30 g/kg) significantly downregulated expression of these genes. These results also suggest that YHPG could ameliorate IFV-induced inflammatory responses which are mediated by the TLR4 and NF-κB signaling pathways.

The major ingredients of YHPG are based upon the classical Ephedra decoction formula, which had been reported to exert antipyretic activity in IFV-infected mice and virus-reducing effects at an early phase of the infection [15]. In this study, HPLC analysis clearly revealed the presence of the major constituents in YHPG. From the literature, we found that the main component of Flos Lonicerae Japonicae, chlorogenic acid, has shown significant antiviral activity in vitro [49, 50]. Glycyrrhizin, which is an active component of *Glycyrrhizae Radix*, may protect mice infected with lethal doses of IFV through the induction of IFN-γ production by T cells [51]. Glycyrrhizin has been reported to inhibit influenza A virus uptake into cells [23]. In addition, the main component of Polygoni Cuspidati Rhizoma, emodin, inhibits the replication of IFV H1N1 in A549 cells [24]. Therefore, we hypothesize that chlorogenic acid, glycyrrhizin and emodin may be the active components of YHPG against IFV. However, additional investigations are required to identify the possible anti-influenza bioactive components in YHPG.

In summary, our results revealed that YHPG can ameliorate inflammatory responses in IFV-infected mice. The antiviral effect of YHPG is associated with the inhibition of

the TLR4-MyD88-TRAF6 signaling pathway and the expression of NF-κB. These findings may provide a possible agent for the treatment of influenza infection in a clinical setting.

Acknowledgment This work was supported by a grant from National Science Foundation of China (No. 81573868), Zhejiang Provincial Natural Science Foundation (Nos. LZ14H270001 and LR13H270001), Zhejiang Province Science and Technology Project (No. 2015C37077). We thank Professor Yi-yu Lu for technical help in the animal experiments and helpful discussion regarding this work.

References

1. Bai GR, Chittaganpitch M, Kanai Y, Li YG, Auwanit W, Ikuta K, Sawanpanyalert P (2009) Amantadine- and oseltamivir-resistant variants of influenza A viruses in Thailand. Biochem Biophys Res Commun 390:897–901
2. Kunisaki KM, Janoff EN (2009) Influenza in immunosuppressed populations: a review of infection frequency, morbidity, mortality, and vaccine responses. Lancet Infect Dis 9:493–504
3. Ruuskanen O, Lahti E, Jennings LC, Murdoch DR (2011) Viral pneumonia. Lancet 377:1264–1275
4. De Clercq E (2006) Antiviral agents active against influenza A viruses. Nat Rev Drug Discov 5:1015–1025
5. Feng E, Ye D, Li J, Zhang D, Wang J, Zhao F, Hilgenfeld R, Zheng M, Jiang H, Liu H (2012) Recent advances in neuraminidase inhibitor development as anti-influenza drugs. ChemMedChem 7:1527–1536
6. Michiels B, Van Puyenbroeck K, Verhoeven V, Vermeire E, Coenen S (2013) The value of neuraminidase inhibitors for the prevention and treatment of seasonal influenza: a systematic review of systematic reviews. PLoS One 8:e60348
7. Downes JE, Marshall-Clarke S (2010) Innate immune stimuli modulate bone marrow-derived dendritic cell production in vitro by toll-like receptor-dependent and -independent mechanisms. Immunology 131:513–524
8. Marchant D, Singhera GK, Utokaparch S, Hackett TL, Boyd JH, Luo Z, Si X, Dorscheid DR, McManus BM, Hegele RG (2010) Toll-like receptor 4-mediated activation of p38 mitogen-activated protein kinase is a determinant of respiratory virus entry and tropism. J Virol 84:11359–11373
9. Martin TR, Wurfel MM (2008) A TRIFfic perspective on acute lung injury. Cell 133:208–210
10. Barton GM (2007) Viral recognition by toll-like receptors. Semin Immunol 19:33–40
11. Imai Y, Kuba K, Neely GG, Yaghubian-Malhami R, Perkmann T, van Loo G, Ermolaeva M, Veldhuizen R, Leung YH, Wang H et al (2008) Identification of oxidative stress and toll-like receptor 4 signaling as a key pathway of acute lung injury. Cell 133:235–249
12. Nhu QM, Shirey K, Teijaro JR, Farber DL, Netzel-Arnett S, Antalis TM, Fasano A, Vogel SN (2010) Novel signaling interactions between proteinase-activated receptor 2 and Toll-like receptors in vitro and in vivo. Mucosal Immunol 3:29–39
13. Wu XN, Yu CH, Cai W, Hua J, Li SQ, Wang W (2011) Protective effect of a polyphenolic rich extract from Magnolia officinalis bark on influenza virus-induced pneumonia in mice. J Ethnopharmacol 134:191–194
14. Li L, Yu CH, Ying HZ, Yu JM (2013) Antiviral effects of modified dingchuan decoction against respiratory syncytial virus infection in vitro and in an immunosuppressive mouse model. J Ethnopharmacol 147:238–244
15. Nagai T, Kataoka E, Aoki Y, Hokari R, Kiyohara H (2014) Alleviative effects of a kampo (a Japanese herbal) medicine "Maoto (Ma-Huang-Tang)" on the Early phase of influenza virus infection and its possible mode of action. Evid Based Complement Alternat Med 2014:187036
16. Hsieh CF, Lo CW, Liu CH, Lin S, Yen HR, Lin TY, Horng JT (2012) Mechanism by which ma-xing-shi-gan-tang inhibits the entry of influenza virus. J Ethnopharmacol 143:57–67
17. Zhang BG, Liu QF (2007) Modern pharmacodynamic research and clinical application of Ephedra decoction. Chin Tradit Pat Med 29:415–422
18. Yang X, Peng WB, Yue XQ (2009) Syndrome differentiation and treatment of Taiyang disease in Shanghan Lun. Zhong Xi Yi Jie He Xue Bao 7:171–174
19. Mantani N, Andoh T, Kawamata H, Terasawa K, Ochiai H (1999) Inhibitory effect of Ephedrae herba, an oriental traditional medicine, on the growth of influenza A/PR/8 virus in MDCK cells. Antivir Res 44:193–200
20. Chen KT, Zhou WL, Liu JW, Zu M, He ZN, Du GH, Chen WW, Liu AL (2012) Active neuraminidase constituents of Polygonum cuspidatum against influenza A(H1N1) influenza virus. Zhongguo Zhong Yao Za Zhi 37:3068–3073
21. Kubo T, Nishimura H (2007) Antipyretic effect of Mao-to, a Japanese herbal medicine, for treatment of type A influenza infection in children. Phytomedicine 14:96–101
22. Kuo KK, Chang JS, Wang KC, Chiang LC (2009) Water extract of Glycyrrhiza uralensis inhibited enterovirus 71 in a human foreskin fibroblast cell line. Am J Chin Med 37:383–394
23. Wolkerstorfer A, Kurz H, Bachhofner N, Szolar OH (2009) Glycyrrhizin inhibits influenza A virus uptake into the cell. Antivir Res 83:171–178
24. Lin CJ, Lin HJ, Chen TH, Hsu YA, Liu CS, Hwang GY, Wan L (2015) Polygonum cuspidatum and its active components inhibit replication of the influenza virus through toll-like receptor 9-induced interferon beta expression. PLoS One 10:e0117602
25. Michaelis M, Geiler J, Naczk P, Sithisarn P, Leutz A, Doerr HW, Cinatl J Jr (2011) Glycyrrhizin exerts antioxidative effects in H5N1 influenza A virus-infected cells and inhibits virus replication and pro-inflammatory gene expression. PLoS One 6:e19705
26. Song W, Si L, Ji S, Wang H, Fang XM, Yu LY, Li RY, Liang LN, Zhou D, Ye M (2014) Uralsaponins M-Y, antiviral triterpenoid saponins from the roots of *Glycyrrhiza uralensis*. J Nat Prod 77:1632–1643
27. He Y, Yu DJ, Zhang YY, Yang JH, Zhou HF, Wan HT (2014) Anti-tussive effect experiment of Yinhua Pinggan granule. Chin Arch Tradit Chin Med 32:2060–2061
28. Wan HT, Yu DJ, Lei Y, Bai HB, Yang JH, Bie XD (2002) Anti-inflammatory and analgesic effects experiment of Jin-Ping-Gan granule. Pharmacol Clin Chin Mater Med 18:39–40
29. Peng HQ, Xu ZM, Wan HT, Yu DJ (2005) Inhibitory effect of Jin-Ping-Gan granule on influenza virus. Zhejiang J Tradit Chin Med 12:87–88
30. Peng XQ, He Y, Zhou HF, Zhang YY, Chen JK, Lu YY, Wan HT (2015) Effects of Yinghuapinggan granule against influenza A/H1N1 virus in vivo. Zhongguo Zhong yao za zhi **(to appear)**
31. Harun A, Vidyadaran S, Lim SM, Cole AL, Ramasamy K (2015) Malaysian endophytic fungal extracts-induced anti-inflammation in Lipopolysaccharide-activated BV-2 microglia is associated with attenuation of NO production and IL-6 and TNF-alpha expression. BMC Complement Altern Med 15:166
32. Livak KJ, Schmittgen TD (2001) Analysis of relative gene expression data using real-time quantitative PCR and the 2(-Delta Delta C(T)) method. Methods 25:402–408
33. Rajasekaran D, Palombo EA, Chia Yeo T, Lim Siok Ley D, Lee TuC, Malherbe F, Grollo L (2013) Identification of traditional

medicinal plant extracts with novel anti-influenza activity. PLoS One 8:e79293
34. Kaiser L, Fritz RS, Straus SE, Gubareva L, Hayden FG (2001) Symptom pathogenesis during acute influenza: interleukin-6 and other cytokine responses. J Med Virol 64:262–268
35. Hayden FG, Fritz R, Lobo MC, Alvord W, Strober W, Straus SE (1998) Local and systemic cytokine responses during experimental human influenza A virus infection. Relation to symptom formation and host defense. J Clin Invest 101:643–649
36. Loo YM, Gale M Jr (2007) Influenza: fatal immunity and the 1918 virus. Nature 445:267–268
37. Yu CH, Yan YL, Wu XN, Zhang B, Wang W, Wu QF (2010) Anti-influenza virus effects of the aqueous extract from Mosla scabra. J Ethnopharmacol 127:280–285
38. Yeo JM, Lee HJ, Kim JW, Lee JB, Park SY, Choi IS, Song CS (2014) Lactobacillus fermentum CJL-112 protects mice against influenza virus infection by activating T-helper 1 and eliciting a protective immune response. Int Immunopharmacol 18:50–54
39. Kawahara T, Takahashi T, Oishi K, Tanaka H, Masuda M, Takahashi S, Takano M, Kawakami T, Fukushima K, Kanazawa H, Suzuki T (2015) Consecutive oral administration of Bifidobacterium longum MM-2 improves the defense system against influenza virus infection by enhancing natural killer cell activity in a murine model. Microbiol Immunol 59:1–12
40. Wiley JA, Cerwenka A, Harkema JR, Dutton RW, Harmsen AG (2001) Production of interferon-gamma by influenza hemagglutinin-specific CD8 effector T cells influences the development of pulmonary immunopathology. Am J Pathol 158:119–130
41. Weiss ID, Wald O, Wald H, Beider K, Abraham M, Galun E, Nagler A, Peled A (2010) IFN-gamma treatment at early stages of influenza virus infection protects mice from death in a NK cell-dependent manner. J Interf Cytokine Res 30:439–449
42. Hussell T, Pennycook A, Openshaw PJ (2001) Inhibition of tumor necrosis factor reduces the severity of virus-specific lung immunopathology. Eur J Immunol 31:2566–2573
43. La Gruta NL, Kedzierska K, Stambas J, Doherty PC (2007) A question of self-preservation: immunopathology in influenza virus infection. Immunol Cell Biol 85:85–92
44. Abdul-Careem MF, Firoz Mian M, Gillgrass AE, Chenoweth MJ, Barra NG, Chan T, Al-Garawi AA, Chew MV, Yue G, van Roojen N et al (2011) FimH, a TLR4 ligand, induces innate antiviral responses in the lung leading to protection against lethal influenza infection in mice. Antivir Res 92:346–355
45. Yamamoto M, Sato S, Hemmi H, Uematsu S, Hoshino K, Kaisho T, Takeuchi O, Takeda K, Akira S (2003) TRAM is specifically involved in the toll-like receptor 4-mediated MyD88-independent signaling pathway. Nat Immunol 4:1144–1150
46. Bradley JR, Pober JS (2001) Tumor necrosis factor receptor-associated factors (TRAFs). Oncogene 20:6482–6491
47. van de Sandt CE, Kreijtz JH, Rimmelzwaan GF (2012) Evasion of influenza A viruses from innate and adaptive immune responses. Viruses 4:1438–1476
48. Lawrence T, Fong C (2010) The resolution of inflammation: anti-inflammatory roles for NF-kappaB. Int J Biochem Cell Biol 42:519–523
49. Wang GF, Shi LP, Ren YD, Liu QF, Liu HF, Zhang RJ, Li Z, Zhu FH, He PL, Tang W et al (2009) Anti-hepatitis B virus activity of chlorogenic acid, quinic acid and caffeic acid in vivo and in vitro. Antivir Res 83:186–190
50. Hu KJ, Wang YH, Wang D (2010) The inhibited effect of chlorogenic acid from the honeysuckle on virus in vitro. Inf Tradit Chin Med 27:27–28
51. Utsunomiya T, Kobayashi M, Pollard RB, Suzuki F (1997) Glycyrrhizin, an active component of licorice roots, reduces morbidity and mortality of mice infected with lethal doses of influenza virus. Antimicrob Agents Chemother 41:551–556